Journal of Power Sources 196 (2011) 6889–6892

Contents lists available at ScienceDirect

Journal of Power Sources

journal homepage: www.elsevier.com/locate/jpowsour

Short communication

State of charge (SOC) dependence of lithium carbonate on $LiNi_{0.8}Co_{0.15}Al_{0.05}O_2$ electrode for lithium-ion batteries

Yoshiyasu Saito [a,*], Masahiro Shikano [b], Hironori Kobayashi [b]

[a] Energy Technology Research Institute, National Institute of Advanced Industrial Science and Technology (AIST) AIST Tsukuba Central 2, 1-1-1 Umezono, Tsukuba, Ibaraki 305-8568, Japan

[b] Research Institute for Ubiquitous Energy Devices, National Institute of Advanced Industrial Science and Technology (AIST) 1-8-31 Midorigaoka, Ikeda, Osaka 563-8577 Japan

ARTICLE INFO

Article history:
Received 17 September 2010
Received in revised form
18 November 2010
Accepted 27 December 2010
Available online 12 January 2011

Keywords:
Lithium-ion battery
FT-IR
ATR
Surface analysis
$LiNi_{0.8}Co_{0.15}Al_{0.05}O_2$
Lithium carbonate

ABSTRACT

Lithium-ion batteries using $LiNi_{0.8}Co_{0.15}Al_{0.05}O_2$ (NCA) as the positive electrode material and hard carbon as the negative electrode material with electrolyte of mixture of ethylene carbonate and dimethyl carbonate containing $LiPF_6$ were fabricated, and the surface materials on the positive electrode were observed by ATR spectroscopy of FT-IR measurement. Lithium carbonate was mainly observed as the surface material and the intensity of IR absorption peaks were depended on state of charge (SOC) of the batteries. The result suggests that the amount of lithium carbonate increases by discharge and decreases by charge.

1. Introduction

Lithium-ion batteries (LIB) have been expected as power sources for hybrid electric vehicle, plug-in hybrid electric vehicle and pure electric vehicle. Long calendar life beyond 10 years is one of important performance required for such usage. Considering improvement the life of LIB and also development the life prediction method, we are studying degradation mechanism of LIB by using various analyzing methods [1–4]. In our past study for LIB using nickel-based oxide as the active material for positive electrode, power fading of the LIB was considered to relate to surface structure change of the positive electrodes from ac impedance analysis. Actually, some variations were detected at the surface region of the material between fresh cells and degraded cells by several surface analysis such as XAFS, HX-PES, FT-IR and so on. Some surface materials such as lithium carbonate, alkyl lithium carbonate, and phosphate were found on the electrode, which were formed by decomposition of electrolyte, and these materials were similar with components of surface film on lithium metal or carbon negative electrode which was commonly called as solid-electrolyte interface after proposal of Peled [5]. Recently, there have been several reports on the results of surface analysis of positive electrode using nickel-based oxide by FT-IR spectroscopy [6–9]. Aurbach et al. reported that pristine active material was covered by lithium carbonate film and it was replaced by solution-related surface species upon storage in electrolyte [6,7]. In the report of Song et al., they concluded that a pre-existing surface layer of lithium carbonate present in their virgin electrode was eliminated just by storing in the electrolyte, and that no lithium carbonate was found on the positive electrode after cycling [9]. On the contrary, formation of lithium carbonate on positive electrode during storage in electrolyte was observed in Ostrovskii et al.'s work [8]. In our past work, we characterized the materials for the electrodes from the cells at SOC (state of charge) = 0% and 100%, and the amount of lithium carbonate were remarkably different between these two SOCs, i.e. more lithium carbonate was observed in the discharged state (SOC = 0%) than the charged state (SOC = 100%) [3]. In addition, the difference between charged and discharged state became larger in the degraded cells after cycling test at 40 °C and below. In this study, we characterize lithium carbonate as a surface material of the positive electrodes of LIB at several SOCs by FT-IR with attenuated total reflection (ATR) method, in order to study the formation and decrease mechanisms of the materials.

2. Experimental

Cylindrical LIB (18650-type) were prepared in which $LiNi_{0.8}Co_{0.15}Al_{0.05}O_2$ (NCA) from Toda Kogyo was selected as

* Corresponding author.
E-mail address: y-saito@aist.go.jp (Y. Saito).

0378-7753/$ – see front matter © 2011 Elsevier B.V. All rights reserved.
doi:10.1016/j.jpowsour.2010.12.098

the active material in the positive electrode. The electrode also contained 7 wt% of polyvinylidene fluoride (PVDF) binder (KF1300, Kureha) and 7 wt% of acetylene black (HS-100, Denki Kagaku Kogyo) as a conductive agent, and had been pasted on a 20 μm thick Al foil as a current collector. The active material in the negative electrode was hard carbon (Carbotron P, Kureha). The electrolyte was purchased from Tomiyama Pure Chemical and which was a mixed solvent of ethylene carbonate (EC) and dimethyl carbonate (DMC) containing 1 mol dm^{-3} $LiPF_6$ where volume ratio of EC and DMC was 1:2. The standard condition of charging we used consisted two phases, where constant current charging of *C*/3 A (157 mA, CC phase) was followed by constant voltage charging at 4.2 V (CV phase) after the battery voltage raised to 4.2 V. Total charging time from CC to CV phases was 3.5 h. On the while, the standard condition of discharging was constant current of *C*/3 A (157 mA) and the cut-off voltage was 2.5 V. The discharging initial capacity *C* was approximately 470 mAh. Standard temperature was 25 °C, and all charging and discharging were carried out at this temperature.

We prepared 14 sample batteries for this study and these were divided into 7 pairs. One pair was disassembled without any history of charge and discharge. The other 6 pairs were disassembled after setting the SOC to 30, 50, 70, 90, or 100%, i.e. two samples were prepared for every SOCs. After the disassembly of the samples in an argon-filled glove box, extracted electrodes were washed in DMC, and dried under vacuum condition. A pristine electrode which had not used in LIB was also supplied for analysis as the reference.

For FT-IR measurement, Magna-560 spectrometer (Nicolet) mounted a multi-angle ATR attachment Seagull (Harrick) with Ge hemisphere crystal (n_1 = 4.0) was used. The mercury-cadmium-telluride (MCT) detector was selected for high sensitive measurement. The sample electrodes were cut into specimen whose size was ca. 12 mm × 12 mm. The electrode surface to analyze was adhered to the ATR crystal. These sampling procedures were also carried out in the glove box. Measurement of ATR was carried out in a small room where temperature was controlled to 25 °C and humidity was 7%. In order to suppress IR absorption of H_2O and CO_2 in the air, N_2 gas was flowed in the apparatus.

ATR spectroscopy is one of surface sensitive analytical methods. In this measurement, sample is pressed to an ATR crystal with high refractive index (n_1), and infrared light is irradiated the sample from the crystal side. If sample is homogeneous with the optical properties α and n_2 as the absorption coefficient and the refractive index, respectively, absorbance *A* is described as

$$A = \log \frac{n_2 {E_0}^2 d_p}{2 n_1 \cos\theta} \alpha \quad (1)$$

where θ is incidence angle of the light, E_0 is strength of electric field of the standing wave at the reflecting interface, and d_p is penetration depth. It is one of advantage of the ATR that we can control d_p, which is related to wavelength (λ) of the radiation, n_1, n_2, and θ and the relationship is well-known as Harrick equation [10],

$$d_p = \frac{\lambda}{2\pi n_1 \sqrt{\sin^2\theta - (n_2/n_1)^2}} \quad (2)$$

and depth profiling of surface materials can be performed with changing these parameters.

3. Results and discussion

Relation of SOC and open circuit voltage (OCV) of a LIB were characterized at first, and the result were summarized in Table 1 and Fig. 1 except for SOC = 0% and 100% where lower and upper limits of voltage were described and plotted instead of OCV. The setting of SOC was carried out by constant current charging of *C*/3 A, and the values of OCVs were measured at 6 h after finish of the charge. Since OCV shows good relation with SOC in the fresh batteries, SOC of batteries can be controlled by constant voltage charging at corresponding value of OCV for enough time. Hence we set SOC of the sample batteries for ATR analysis by constant voltage charging for about 30 min following constant current charging of *C*/3 A.

Lithium composition *x* of the positive electrode material $Li_xNi_{0.8}Co_{0.15}Al_{0.05}O_2$ was analyzed by ICP measurement for the extracted electrodes, and the result was plotted in Fig. 2 as a function of SOC. Good linearity of the plot suggests SOC of the samples can be actually controlled by constant voltage charging.

Table 1
State of charge (SOC) of the sample batteries and composition *x* in $Li_xNo_{0.80}Co_{0.05}Al_{0.05}O_2$ as the positive electrode material.

SOC (%)	OCV (V)	Code of LIB	Lithium composition *x*
0	2.500[a]	1008	0.802
		1022	0.796
30	3.372	1012	0.677
		1013	0.674
50	3.667	1014	0.582
		1015	0.557
70	3.876	1017	0.479
		1019	0.484
90	4.010	1026	0.397
		1028	0.394
100	4.100[b]	1016	0.338
		1030	0.340
Non-cycled	–	1042	1.060
		1043	1.060
Pristine	–	S091009	1.060

[a] Lower limit of voltage (cut-off voltage in discharging).
[b] Upper limit of voltage (cut-off voltage in charging).

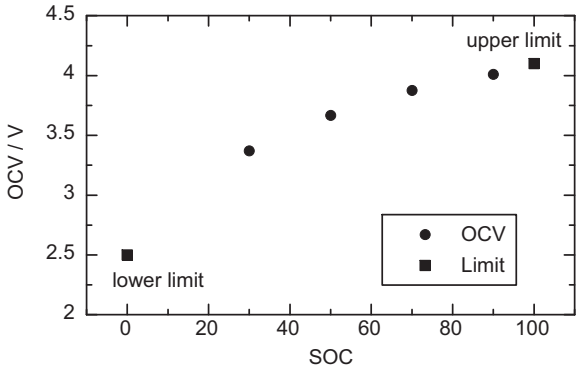

Fig. 1. Relation of open circuit voltage (OCV) and state of charge (SOC) in a lithium-ion battery.

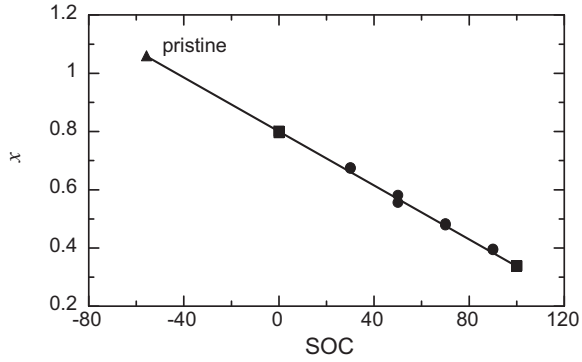

Fig. 2. Relation of composition *x* in $Li_xNi_{0.80}Co_{0.15}Al_{0.05}O_2$ and state of charge (SOC) in a lithium-ion battery.

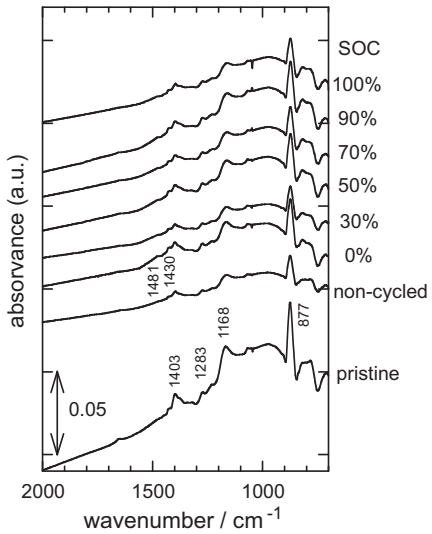

Fig. 3. ATR spectra of the positive electrodes of lithium-ion batteries at various states of charge (SOCs).

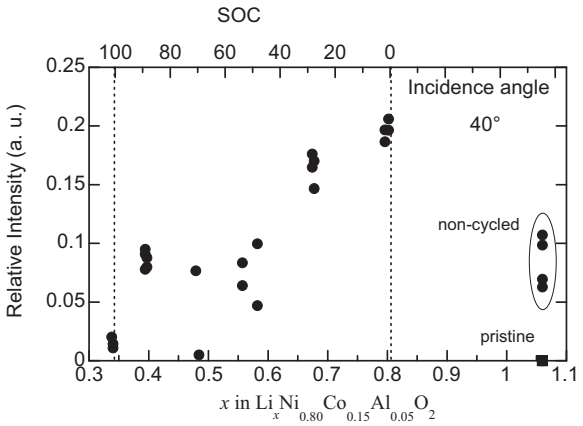

Fig. 4. Relative intensity of peak at 1481 cm^{-1} of Li_2CO_3 to peak at 1403 cm^{-1} of PVDF depending on composition x in $Li_xNi_{0.80}Co_{0.15}Al_{0.05}O_2$ and states of charge (SOCs).

Fig. 3 shows ATR spectra of the positive electrodes when the incidence angle is 40°. The penetration depth d_p depends on wavenumber, and it is ca. 762 nm for 1000 cm^{-1} and ca. 508 nm for 1500 cm^{-1}, if the refractive index of sample is 1.5 which is general value for organic materials. A lot of peaks were observed in all samples including the pristine electrode. Peaks in the spectrum of the pristine electrode could be attributed to IR absorption bands of the PVDF binder, because there is no surface material as decomposition products of the electrolyte. Actually, the profile of the spectrum is similar with that of PVDF. In the reports of Aurbach [6,7] and Song [9], IR bands of lithium carbonate were observed even in pristine samples. Matsumoto et al. proposed that a nickel oxide based electrode material, $LiNi_{1-x-y}Co_xAl_yO_2$, reacted with atmospheric CO_2 even at room temperature, and the layer of lithium carbonate was formed on the surface of the material [11]. Aurbach's and Song's samples would have been affected by CO_2. The ATR spectra of the electrodes extracted from LIBs in Fig. 3 were also similar with that of the pristine sample. However, slight difference was observed at around 1430 cm^{-1} and 1480 cm^{-1}. Those two bands could be attributed to absorption bands of carbonyl (C=O) stretching vibration in lithium carbonate (Li_2CO_3) as same as our past study [3]. In general, peak strength shows linear relation with concentration of the material in FT-IR spectroscopy. However, since the sample electrodes were not homogeneous bulk material, measured value of peak intensity varied with sampling position due to surface roughness even in identical sample. In such sample, peak strength of IR bands depends on contact area between the ATR crystal and the samples. Contact pressure between sample and ATR crystal also affected the peak strength. Hence it is difficult to discuss about variation of intensity for ATR peaks of lithium carbonate depending on SOC if there is no adequate internal standard. Fortunately, in our sample electrodes contained PVDF binder. If PVDF dispersed in the electrode homogeneously, we might be use the PVDF as the internal standard for quantitative analysis of surface materials. Considering the penetration depth depends on wavenumber, we select IR band of PVDF at 1403 cm^{-1} as the standard which is close to IR bands of lithium carbonate. Fig. 4 shows the relative intensity of ATR peak at 1480 cm^{-1} for lithium carbonate depending on lithium composition x in $Li_xNi_{0.8}Co_{0.15}Al_{0.05}O_2$, where larger x corresponds to lower SOC. The sample from LIBs without cycling history, i.e. samples 1042 and 1043, shows small peaks of lithium carbonate suggesting small amount of lithium carbonate may be formed on the positive electrode by just contacting the electrolyte with the electrode. This is same result with Ostrovskii et al.'s work [8] except that P-, O- and F-containing compounds have been formed more predominately than lithium carbonate, and their pristine sample also has not show IR bands of lithium carbonate remarkably. It seems that pristine sample which is not containing lithium carbonate as impurity shows formation of lithium carbonate by contact with electrolyte. Although Aurbach et al. had observed $ROCO_2Li$ on their electrode after cycling [6,7], we could not obtain remarkable peaks for $ROCO_2Li$ in our samples. Song et al. mentioned that surface layer on NCA was easily removed by rinsing with DMC [9]. In our samples, some surface species formed during SOC setting might be removed in the washing process by DMC.

In Fig. 4, it was clear that the sample from the LIB at lower SOC such as 0% and 30% shows strong peaks of lithium carbonate. This lithium carbonate was thought to be formed during discharging process of the batteries. On the while, relative intensity of the peak is almost same as that of the electrodes from non-cycled batteries if SOC is 50% or 90%. In addition, the peak is not remarkable for the some samples at SOC = 70% or 100%. Since the SOC of the batteries had been set by charging from SOC = 0%, it was suggested that the amount of lithium carbonate decreased during the charging.

We also prepared LIB using mixture of propylene carbonate (PC) and diethyl carbonate (DEC) as the electrolytic solvent. However, any remarkable peaks of lithium carbonate were not observed in ATR measurement of the positive electrodes. In our past report [3] using mixed solvent of PC and DMC, lithium carbonate was observed. Hence the main source of lithium carbonate formation during discharge could be DMC. We had reported that lithium deficient cubic phase was observed at the surface of NCA electrodes of degraded lithium-ion batteries by XAFS analysis [1]. Aurbach et al. speculated a formation mechanism of $ROCO_2Li$ on $LiNiO_2$ electrode as surface nucleophilic reaction between $LiNiO_2$ and EC or DMC [6,7]. The direct reaction between NCA and DMC may also occur in our samples at lower SOC region, and it does not produce $ROCO_2Li$ but lithium carbonate on the surface and lithium deficient cubic phase in NCA, as follows;

$$LiNi_{0.8}Co_{0.15}Al_{0.05}O_2\,(\text{hexagonal}) + y\,CH_3OCO_2CH_3 \rightarrow Li_{1-2y}Ni_{0.8}Co_{0.15}Al_{0.05}O_2\,(\text{cubic}) + y\,Li_2CO_3 + 2y\,CH_3{}^+ \quad (3)$$

Another possibility of lithium carbonate formation is side-reaction during discharge where the surface of NCA may affects as a catalyst. However, this mechanism cannot explain existence of lithium carbonate in the non-cycled samples.

For the decrease of the lithium carbonate during charging, two possible mechanisms should be considered; electrochemical

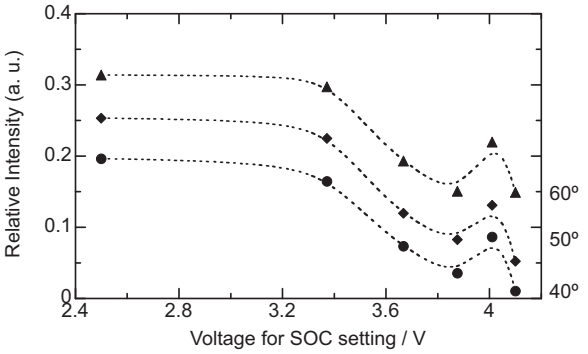

Fig. 5. Relative intensity of peak at 1481 cm^{-1} of Li_2CO_3 to peak at 1403 cm^{-1} of PVDF depending on voltage for SOC setting and incidence angle in ATR measurement.

decomposition and runoff by the stress in the volume change of the active electrode material or affected by formation of some the other materials on the electrode surface however we could not observe them in this study. Variation of peak intensity of lithium carbonate depending on SOC had been also observed in positive electrodes of cycled batteries in our past study [3]. The repetition of formation and elimination of lithium carbonate at the electrode surface during cycling may cause capacity fade of the battery if lithium ion intercalated in NCA was consumed to form the lithium carbonate as like Eq. (3), and also cause power fade with growing up the lithium deficient cubic phase in NCA.

As mentioned above, the incidence angle is one of parameters to control the penetration depth in ATR. Fig. 5 shows relative intensity of peak at 1481 cm^{-1} measured by several incidence angles as a function of voltage for SOC setting. The standard peak for the normalization was the band at 1403 cm^{-1} of PVDF as like Fig. 4. The penetration depths were assumed to be 515 nm for 40°, 402 nm for 50°, and 344 nm for 60°. Apparently higher angle give stronger relative intensity in Fig. 5. This result indicates that lithium carbonate disperses in shallow region of the surface of the positive electrodes compared with PVDF. Since the layer including PVDF is not limited in surface region but the whole electrode, this result suggests lithium carbonate has been mainly formed at the electrode surface. In Fig. 5, a small peak is observed at around 4 V (SOC = 90%). The reason why the peak increases at 4 V and decreases at 4.1 V again during charging is indefinite from only the present data. It may be related to surface structure of the NCA.

4. Conclusion

Observation of the surface material was carried out by ATR measurement for the positive electrodes of lithium-ion batteries using NCA as the active material. The IR absorption peaks of lithium carbonate were mainly observed on the electrodes, and the intensity depended on SOC of the batteries. The result suggests that the amount of lithium carbonate increases by discharge and decreases by charge.

Acknowledgment

This work was supported by “the Lithium-ion and Excellent Advanced Batteries Development (Li-EAD) project” of the New Energy and Industrial Technology Development Organization (NEDO) in Japan.

References

[1] H. Kobayashi, M. Shikano, S. Koike, H. Sakaebe, K. Tatsumi, J. Power Sources 174 (2007) 380–386.
[2] M. Shikano, H. Kobayashi, S. Koike, H. Sakaebe, E. Ikenaga, K. Kobayashi, K. Tatsumi, J. Power Sources 174 (2007) 795–799.
[3] M. Rahman, Y. Saito, J. Power Sources 174 (2007) 889–894.
[4] Y. Saito, M. Rahman, J. Power Sources 174 (2007) 877–882.
[5] E. Peled, J. Electrochem. Soc. 126 (1979) 2047–2051.
[6] D. Aurbach, B. Markovsky, M.D. Levi, E. Levi, A. Schechter, M. Moshkovich, Y. Cohen, J. Power Sources 81 (82) (1999) 95–111.
[7] D. Aurbach, K. Gamolsky, B. Markovsky, G. Salitra, Y. Gofer, U. Heider, R. Oesten, M. Schmidt, J. Electrochem. Soc. 147 (2000) 1322–1331.
[8] D. Ostrovskii, F. Ronci, B. Scrosati, P. Jacobsson, J. Power Sources 94 (2001) 183–188.
[9] S.-W. Song, G.V. Zhuang, P.N.Jr. Ross, J. Electrochem. Soc. 151 (2004) A1162–A1167.
[10] N.J. Harrick, Internal Reflection Spectroscopy, Wiley-Interscience, New York, 1967.
[11] K. Matsumoto, R. Kuzuo, K. Takeya, A. Yamanaka, J. Power Sources 81 (82) (1999) 558–561.